ACS APPLIED MATERIALS & INTERFACES

Research Article

www.acsami.org

Synthesis of Polydopamine-Coated Magnetic Graphene for Cu^{2+} Immobilization and Application to the Enrichment of Low-Concentration Peptides for Mass Spectrometry Analysis

Man Zhao, Chunhui Deng,* and Xiangmin Zhang

Department of Chemistry and Institutes of Biomedical Sciences, Fudan University, Shanghai 200433, China

Supporting Information

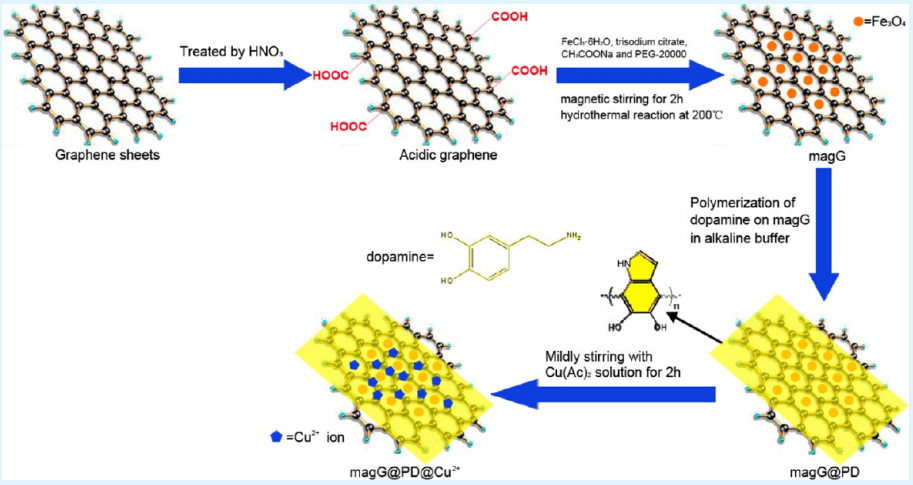

ABSTRACT: In this work, Cu^{2+}-immobilized magnetic graphene@polydopamine (magG@PDA@Cu^{2+}) composites were synthesized for the first time. Magnetic graphene prepared via a hydrothermal reaction were easily encapsulated by a layer of polydopamine through the oxidative polymerization of dopamine in alkaline buffer, and it was conveniently modified with Cu^{2+} ions afterward. The as-prepared magG@PDA@Cu^{2+} composites were endowed with strong magnetic responsivness, excellent dispersibility and biological compatibility. We applied the novel nanocomposites to the enrichment and identification of low-concentration standard peptides, peptides in standard protein digestions, endogenous peptides in human urine and serum. The enriched peptides were eluted and analyzed by matrix-assisted laser desorption/ionization time-of-flight mass spectrometry (MALDI-TOF MS). The magG@PDA@Cu^{2+} composites were proved to exhibit great affinity to both hydrophobic and hydrophilic peptides, thus providing a rapid and facile approach to the extraction of low-concentration peptides. Notably, peptides at an extremely low concentration of 10 pM could be detected by MALDI-TOF MS after enrichment with magG@PDA@Cu^{2+} composites. The results demonstrated that the magG@PDA@Cu^{2+} composite is a promising candidate for the enrichment of low-abundance peptides for mass spectrometry analysis.

KEYWORDS: *low-concentration peptides, enrichment, MALDI-TOF mass spectrometry, magnetic graphene@polydopamine, affinity interaction*

INTRODUCTION

Peptide mapping based on matrix-assisted laser desorption/ionization time-of-flight mass spectrometry (MALDI-TOF MS) along with bioinformatics is an indispensible tool in proteomic analysis.[1−4] The enrichment of peptides is prior to MALDI-TOF MS analysis in most cases involving peptides identification, because peptides extracted from biological samples are not only expressed at extremely low concentrations (less than 1 nM) but they also suffer from strong interference with highly abundant proteins/peptides as well as contaminants like buffer salts or surfactants introduced into the sample during the pretreatment process. Moreover, many of the biologically active peptides such as hormones, cytokines, which are considered to contain potential biomarkers for recording the physiological and pathological states of human beings,[5,6] are usually low-abundance peptides. Therefore, great efforts have been devoted to the development of simple, rapid, convenient and universal enrichment protocols.

Over the past decade, magnetic nanomaterials have been widely utilized to settle this issue. In our previous works, various core−shell structured magnetic nanocomposites with hydrophobic surfaces were synthesized to enrich low-concentration

Received: September 23, 2013
Accepted: November 27, 2013
Published: November 27, 2013

Scheme 1. Synthetic Route of magG@PDA@Cu^{2+} Nanocomposites

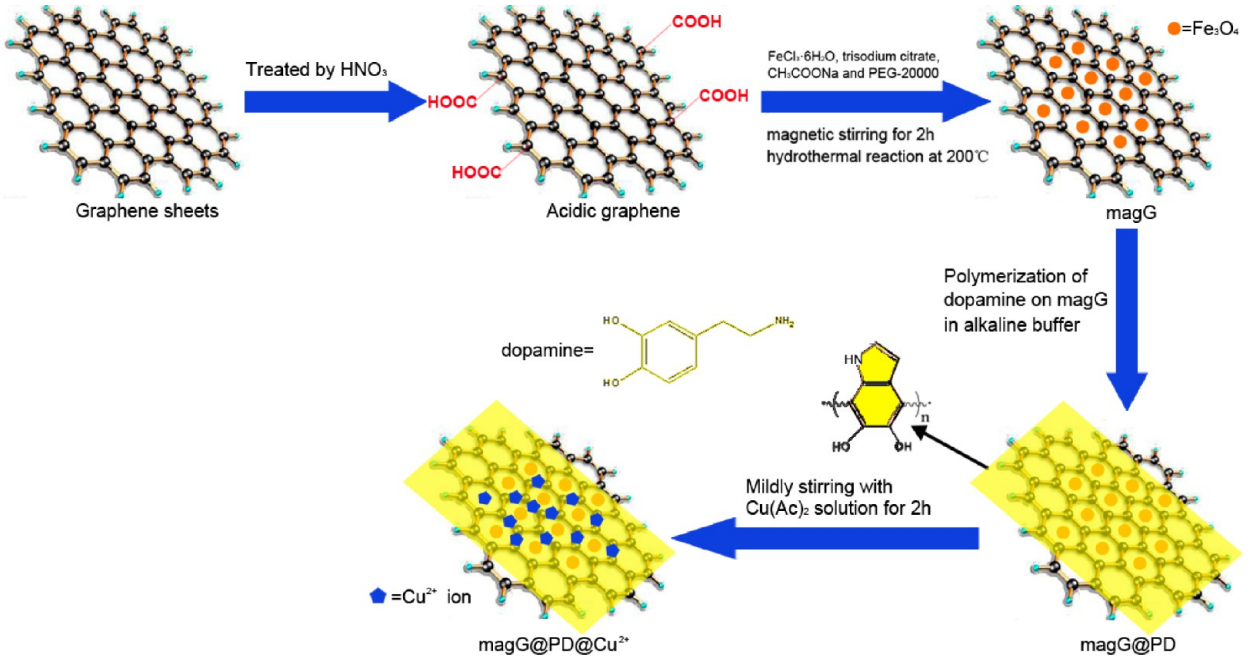

peptides.[7−10] However, the class of hybrid materials encapsulated by hydrophobic shells can merely capture hydrophobic peptides. Surface modification with metal ions is regarded as an ideal alternative for the functionalization with *n*-alkyl chains. Metal ions enrich peptides through their affinity to carboxyl and amino groups. Among these metal ions, for enrichment purposes, copper ions were the most favored because they have strong affinity to both hydrophilic and hydrophobic peptides. We had successfully applied Cu^{2+}-immobilized magnetic microspheres to the enrichment of peptides previously.[11] The smart material combined the merits of the high magnetic responsiveness of Fe_3O_4 cores and the specific affinity of Cu^{2+} ions toward peptides, facilitating and accelerating the enrichment and separation procedures. The Cu^{2+} ions can be immobilized on substrates and can capture amino acid chains of the peptides via coordination bonds, and after enrichment the peptides can be released through the disruption of coordination bonds by using an eluting reagent. Nevertheless, the substrates (such as Fe_3O_4 particle) used to immobilize Cu^{2+} ions often suffer from limited specific surface area and poor solubility.

Since its discovery in 2004,[12] graphene has stimulated a tremendous amount of research interest in the area of materials science and nanotechnology. Thanks to its ultrahigh surface area (2630 $m^2\ g^{-1}$)[13] and outstanding feasibility of associating with metals, polymers and silica,[14−16] graphene-based materials have been widely applied to analytical chemistry in recent years.[17−20] Magnetic graphene was prepared in 2009 for the first time[21] and has driven the development of carbon-based composite nanomaterials ever since. Integrated with magnetic particles, the graphene nanosheet has become a promising platform in the analyses of proteins, peptides and many other biological molecules. Up to now, magnetic graphene composites have been successfully employed in the effective enrichment of proteins[22] and the selective enrichment of hydrophobic peptides for MALDI-TOF MS analysis.[23]

Dopamine is a neurotransmitter in the catecholamine and phenethylamine families that plays a number of important roles in the brains and bodies of animals. Polydopamine (PDA) was synthesized after dopamine polymerized in alkaline buffer.[24] Owing to PDA's unique properties such as excellent dispersibility in water and extraordinary biocompatibility, the PDA coating strategy has turned out to be an efficient approach in modifying substrates. PDA's successful adhesion to varieties of solid substrates,[25−28] especially carbon nanotubes,[29−32] greatly enhanced their solubility and blood compatibility and tailored them to satisfy the requirements of clinical applications. Recently, the PDA coating protocol has been successfully introduced into the encapsulation of living cells,[33] immobilizing endothelial cells[34] and in vivo cancer therapy.[35] In addition, PDA exhibits potential to immobilize metal ions (e.g., Ti^{4+}, Fe^{3+}, Cu^{2+}).[36−38] Hence, we propose that PDA is a promising candidate for the substrate of magnetic graphene to immobilize Cu^{2+} ions for the enrichment of low-abundance peptides.

Herein we report a facile synthesis strategy of polydopamine-coated magnetic graphene with the surface immobilization of Cu^{2+} ions (designated as magG@PDA@Cu^{2+}). The synthesis strategy is shown in Scheme 1. First, Fe_3O_4 magnetic particles were deposited on the graphene sheets treated with HNO_3 via a simple hydrothermal reaction.[39] Then, the magnetic graphene sheets were easily wrapped by a layer of polydopamine after being dispersed in an alkaline solution (10 mM Tris, pH = 8.5) of dopamine hydrochloride, mildly stirring at room temperature, which triggered the polymerization of dopamine. A considerable amount of copper ions was deposited on the PDA layer by mechanically stirring the obtained magG@PDA composites with the $Cu(Ac)_2$ solution at room temperature. Thanks to the ultrahigh specific surface area of the graphene substrate, the novel material can immobilize a great amount of Cu^{2+} ions, thus increasing its capability to enrich peptides. Pristine graphene is highly hydrophobic and unsuitable for application in a biological environment, whereas being encapsulated with polydopamine enhanced its dispersibility in water and made it a suitable candidate for the treatment of biological samples. The nanocomposite marries the brilliant features of magnetic microspheres, polydopamine and Cu^{2+} ions, and is a promising

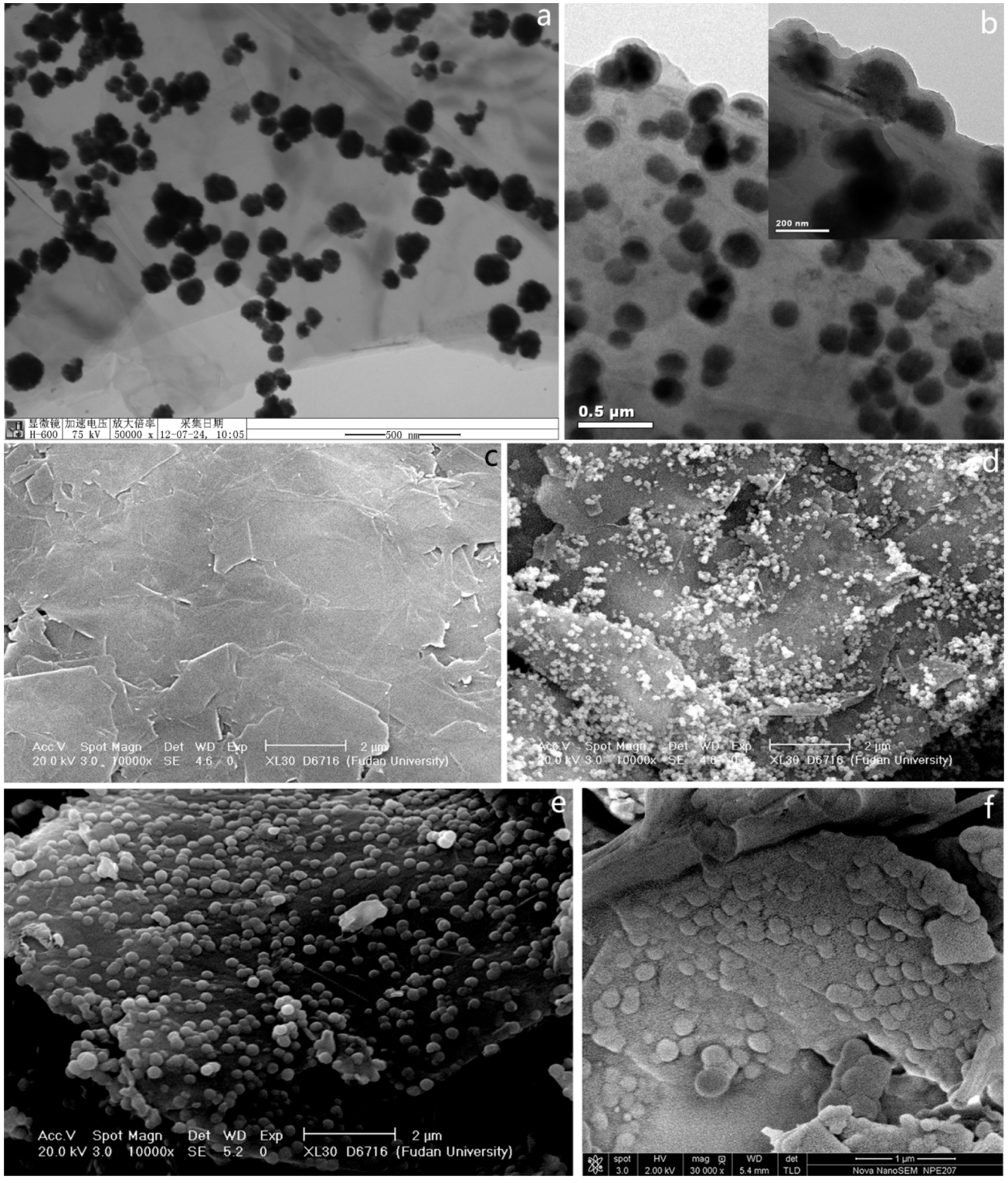

Figure 1. TEM images of (a) magG and (b) magG@PDA. The SEM images of (c) HNO_3-treated graphene, (d) magG, (e) magG@PDA and (f) magG@PDA@Cu^{2+}.

adsorbent for the enrichment of low-concentration peptides by mass spectrometry detection.

RESULTS AND DISCUSSION

The structures, morphologies, components and other chemical properties of the as-synthesized polydopamine-modified magnetic graphenes (designated as magG@PDA) and magG@PDA@Cu^{2+} nanocomposites were characterized by employing various techniques. The TEM images of magG before and after being coated with PDA are shown in Figure 1a,b. As we can see from the image, before coating, the single-layer graphene sheets were occupied with plenty of magnetite beads. After being wrapped by PDA, layers of PDA with a thickness of around 25 nm were visible outside the composites, especially on the margin

of the magnetite microspheres. No free PDA particles were observed in the TEM image of the mag@PDA composites, which implies a heterogeneous nucleation of PDA during the polymerization process.

The SEM images images of HNO_3-treated graphene, Fe_3O_4-mofied G (designated as magG), magG@PDA and magG@PDA@Cu^{2+} composites are displayed in Figure 1c–f. Figure 1c suggests that the acidic graphene has a single-layer structure with characteristic crumpled surface. Figure 1d indicates that considerable magnetite beads were deposited on the surface of the graphene sheets after the hydrothermal reaction was performed. As is shown in Figure 1e, the magnetite beads became larger in diameter after encapsulation with PDA. As a result of interaction with the $Cu(Ac)_2$ solution, the magnetite beads in the resulting products became blurred (Figure 1f) because the magnetic microspheres were further embedded in the coating of Cu^{2+} ions.

Fourier transform infrared spectroscopy (FT-IR) was employed to characterize the G sheets treated by nitric acid, magG, magG@PDA and magG@PDA@Cu^{2+} (Figure 2). In the

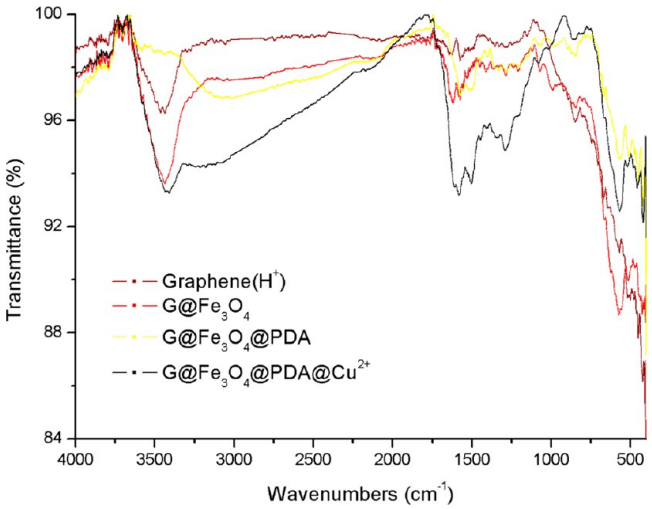

Figure 2. The FT-IR spectra of HNO_3-treated graphene, magG, mag@PDA and magG@PDA@Cu^{2+}.

spectrum of acidic graphene, the absorption band at 3434 cm^{-1} is assigned to the O—H stretching vibration and the bands at 1641 and 1625 cm^{-1} are assigned to the C═O stretching vibration of carboxyl groups. After being decorated with Fe_3O_4 magnetic microspheres, the peak at 575 cm^{-1} assigned to the Fe—O—Fe vibration of magnetite emerged. And after being coated with PDA, there arise many new peaks in the spectra of the magG@PDA and magG@PDA@Cu^{2+} composites. The absorption bands at 3409 and 1606 cm^{-1} can be assigned to the aromatic O—H stretching vibration and the aromatic C═C stretching vibration, respectively. The broad and weak absorption bands within the range between 1600 and 1500 cm^{-1} originated from the benzene ring structure. The absorption bands from 1400 to 600 cm^{-1} contain a $-CH_2$ bending vibration (1340 cm^{-1}), a C—O—H asymmetric bending vibration (1288 cm^{-1}), a C—O asymmetric vibration (1240 cm^{-1}), a C—N stretching vibration (1144 cm^{-1}) and an Ar–H bending vibration assigned to 1,2,4-substituted aromatic compounds (845 and 754 cm^{-1}). These results confirm that graphene sheets have been successfully encapsulated by PDA polymers via the facile oxidative polymerization method.

The Raman spectra of the four compounds mentioned above are shown in Figure 3. In the spectrum of HNO_3-treated

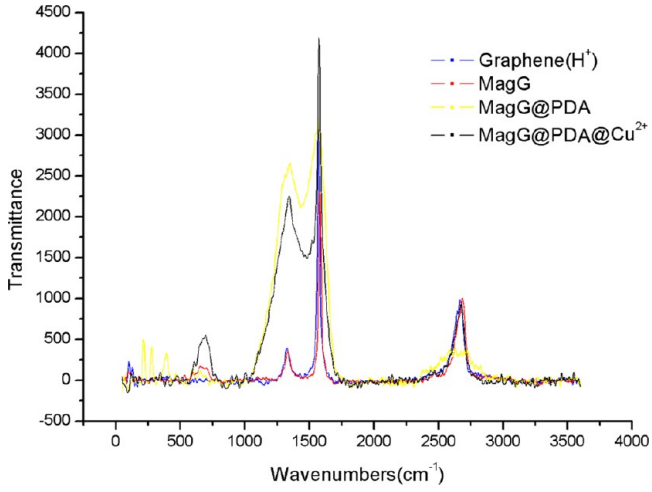

Figure 3. Raman spectra of HNO_3-treated graphene, magG, mag@PDA and magG@PDA@Cu^{2+}.

graphene, the three strong characteristic peaks at 1325, 1570 and 2667 cm^{-1} are attributed to the D, G and 2D mode of graphene. However, in the spectrum of magG, the emergence of the peak at 709 cm^{-1} is attributed to Fe–O vibration, which also indicates that magnetic microspheres were successfully combined with the graphene sheets. In the spectra of magG@PDA and magG@PDA@Cu^{2+}, all the characteristic peaks remain in their original positions but became slightly broadened. The changes in the Raman spectra are due to the existence of PDA polymers because PDA gives broader bands at the same position as graphene according to a previous report.[30] Additionally, the composites modified with PDA give a new peak at around 815 cm^{-1}, resulting from the stretching and deformation of aromatic rings and the generation of aliphatic C–C and C–O bonds. In conclusion, the Raman spectra of magG@PDA and magG@PDA@Cu^{2+} show the combined features of magG and PDA, which are in accordance with the investigation by FT-IR spectra.

X-ray diffraction patterns for magG and magG@PDA present an intense peak at 26° (Figure S1, Supporting Information), indicative of a large number of graphitic layers in the compound. And peaks near 30.1, 35.5, 43.1, 53.5, 57.0 and 62.6° correspond to the specific (220), (311), (400), (422), (551) and (440) planes of Fe_3O_4 lattice. The energy dispersive X-ray analysis (EDXA) (Figure S2a, Supporting Information) of the illuminating electron beams on the obtained magG@PDA@Cu^{2+} reveals the containment of O and Cu elements, and the Cu element accounts for 23.75% of the total weight of the two elements. To prove an even distribution of Cu^{2+} ions throughout the PDA matrix, we performed EDX analysis on two other regions on the surface of magG@PDA@Cu^{2+}, and the results exhibited a close proportion of 23.66% and 24.08% for the Cu element (Figure S2b,c, Supporting Information).

The zeta potential measurements were carried out for HNO_3-treated graphene, magG, magG@PDA and magG@PDA@Cu^{2+} in deionized water. As is implied by Figure S3 and Table S1 (Supporting Information), the zeta potential of HNO_3-treated graphene is −27.5 mV with plenty of negatively charged carboxylic groups.[39] After modification with magnetic particles, it increased to −13.5 mV because the surface turned to being positively charged with the generation of Fe_3O_4. After coating

with PDA, the potential decreased to −25.5 mV with the emergence of negatively charged acidic catechol hydroxyls.[40] And after $Cu(Ac)_2$ was mixed into the solution, it eventually increased to −17.7 mV, resulting from the immobilized Cu^{2+} ions. Therefore, the zeta potential characterization confirmed the generation of new species on the surface of the graphene-cored composites after each step of the synthesis.

Nitrogen sorption was performed to study the surface area of magG@PDA@Cu^{2+}. As is displayed in Figure 4, the BET surface area was calculated to be 107.233 $m^2\ g^{-1}$, implying a relatively high surface area. In contrast, the BET surface area of Fe_3O_4@SiO_2@Cu^{2+} was only 85 $m^2\ g^{-1}$. The results suggest that the introduction of graphene considerably increased the specific surface area of the material.

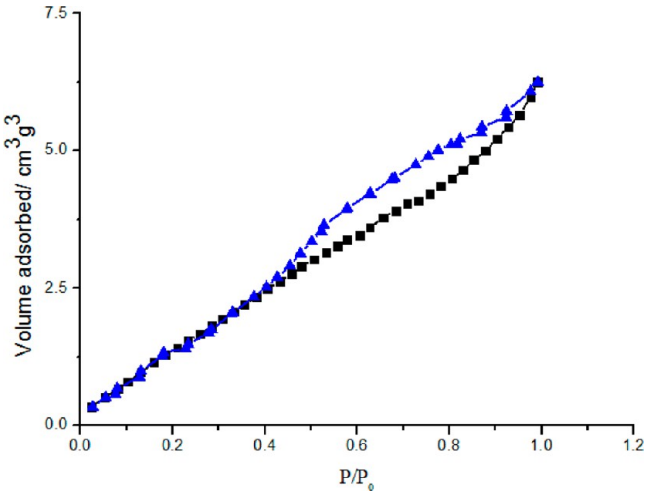

Figure 4. N_2 sorption−desorption isotherms of the as-prepared magG@PDA@Cu^{2+} nanocomposites measured at 77 K.

Before the enrichment of peptide samples, magG@PDA@Cu^{2+} nanocomposites were suspended in deionized water to prepare a dispersion at the concentration of 10 mg/mL. To display the excellent dispersibility of magG@PDA@Cu^{2+}, magG@PDA@Cu^{2+} composites and pristine graphene were dispersed in deionized water separately. After being vibrated with the help of a vortex for a few seconds and being ultrasonicated for 3 min, clear and homogeneous dispersions with no sedimentation were obtained for each graphene sheet (Figure S4a, Supporting Information). Judging from Figure S4b (Supporting Information), dispersion of untreated graphene began to precipitate after being set aside for 10 min while magG@PDA@Cu^{2+} still kept good dispersity. And after 3 h, pristine graphene completely precipitated at the bottom of the vial. In contrast, magG@PDA@Cu^{2+} dispersion remained highly dispersible over time (Figure S4c, Supporting Information). Notably, the samples were allowed to rest for 3 days at room temperature without agitation (Figure S4d, Supporting Information). Due to the presence of numerous hydrophilic moieties such as hydroxyl and amine groups, the successful grafting of PDA greatly improves the dispersibility of the material.

To study the enrichment effect of magG@PDA@Cu^{2+} on low-concentration peptides, we firstly used a standard peptide

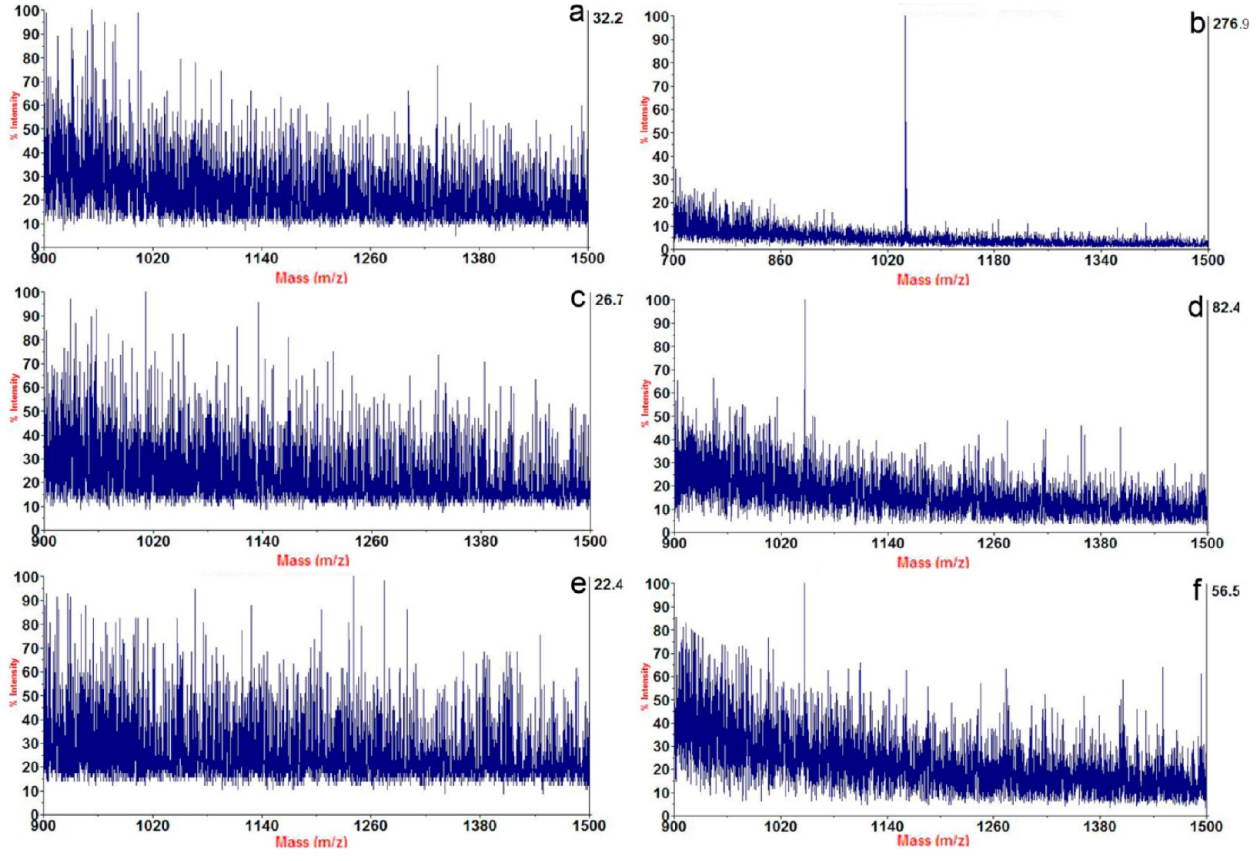

Figure 5. MALDI-TOF mass spectra of Angiotensin II aqueous solution at concentration: (a) 50 pM, (c) 20 pM and (e) 10 pM without any treatment and (b) 50 pM, (d) 20 pM and (f) 10 pM after enrichment with magG@PDA@Cu^{2+}.

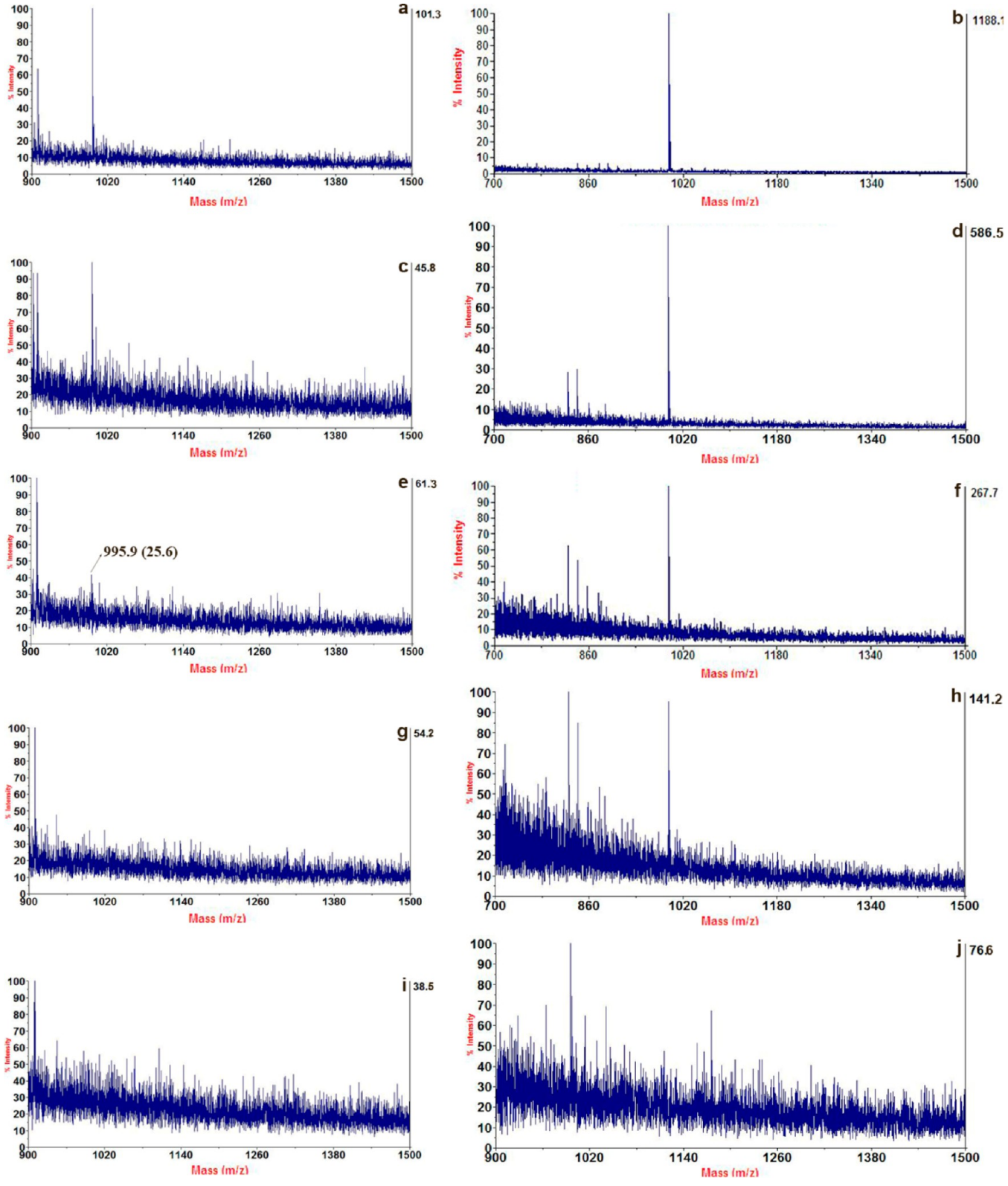

Figure 6. MALDI-TOF mass spectra of microcystin-LR aqueous solution at concentration: (a) 10 nM, (c) 5 nM, (e) 2 nM, (g) 1 nM and (i) 0.5 nM without any treatment and (b) 10 nM, (d) 5 nM, (f) 2 nM, (h) 1 nM and (j) 0.5 nM after enrichment with magG@PDA@Cu^{2+}.

Angiotensin II (DRVYIHPF, M_r = 1046.2 Da, isoelectric point (pI) = 6.74) as a model. The MS spectra of Angiotensin II aqueous solutions at the concentration of 50, 20 and 10 pM are shown in Figure 5a,c,e. When the concentration of Angiotensin II was lower than 100 pM, it could no longer be detected by MALDI-TOF MS. However, after incubation with magG@PDA@Cu^{2+} for 30 min under continuous agitation and subsequent separation for 5 s with the help of a magnet, followed by a three-cycle rinse with deionized water and elution for 10 min by 0.4 M ammonia, the peak of Angiotensin II could

successfully be identified with a signal-to-noise (S/N) ratio up to 276.9, 82.2 and 56.5 (Figure 5b,d,f). The detection limit of the novel sample pretreatment method has reached 10 pM, which was not achieved in several similar reports such as the employment of oleic acid-functionalized magnetite nanoparticles (200 pM),[41] C60-functionalized magnetic silica microspheres (about 500 pM)[10] in the enrichment of low-concentration peptides. Thus, the newly developed approach attained higher sensitivity in the enrichment of Angiotensin II than those of the widely known ones. In addition, the MS spectra of Angiotensin II aqueous solutions with various concentrations from 10 nM to 100 pM are also shown in Figure S5a,c,e,g,i,k,m (Supporting Information). Angiotensin II at the concentration of 10 nM, 5 nM, 2 nM, 1 nM, 0.5 nM, 200 pM and 100 pM could be scarcely detected with a signal-to-noise (S/N) ratio of 721.6, 328.6, 258.8, 199.6, 99.6, 51.4 and 47.5. After an enrichment procedure, the S/N ratio increased to 12 000, 4716.9, 2854.1, 2464.7, 1384.3, 904.3 and 444.7, respectively. The enrichment factor of the pretreatment approach ranged from 10 to 18, which exhibited remarkable enrichment efficiency and a wide linear range.

To prove the effect of immobilized Cu^{2+} ions on the enrichment efficiency, comparative experiments were carried out by applying magG@PDA sheets before and after surface modification with Cu^{2+} ions as the adsorbents for Angiotensin II. As is revealed by Figure S6 (Supporting Information), magG@PDA achieved an enrichment factor of around 5 in the range from 10 to 0.5 nM, only half of the enrichment factors of magG@PDA@Cu^{2+} at most, suggesting that the immobilized Cu^{2+} ions enable the material to capture the peptides efficiently.

Similarly, magG@PDA@Cu^{2+} also proved to be effective for the enrichment of a hydrophilic standard peptide microcystin-LR (MC-LR) in aqueous solution. The peptide was barely detectable at a concentration of 10, 5 and 2 nM (Figure 6a,c,e), and when the concentration decreased to 1 nM or even lower, it was hard to detect (Figure 6g,i). Treatment with magG@PDA@Cu^{2+} resulted in a distinct increase in the S/N ratio up to 1188.1, 586.5, 267.7, 141.2 and 76.6 (Figure 6b,d,f,h,j, respectively).

Another merit of the as-prepared polydopamine-based composite resides in that it could enrich hydrophilic and hydrophobic peptides without discrimination. Therefore, magG@PDA@Cu^{2+} can serve as a versatile adsorbent in the extraction of more complex systems with a variety of peptides and can enrich peptides universally. Bovine serum albumin (BSA), horse heart myoglobin (MYO) and cytochrome c (Cytc) tryptic digest solutions (10 nM) were used to evaluate the universality of this enrichment technique. When no condensation procedures were conducted, only six assignable peptides (m/z = 927, 1193, 1249, 1479, 1567 and 1640), three assignable peptides (m/z = 748, 1606 and 1981) and one assignable peptide (m/z = 1434) could be observed in the BSA MYO and Cytc digest with weak signals (Figures 7a, S7a and S8a, Supporting Information), for the sake of low concentrations of the peptides. After each sample was treated with magG@PDA@Cu^{2+}, the number of matched peptides for the tryptic digests had grown to 9, 11 and 6, respectively. The MS peak with the highest S/N ratio (m/z = 1193) of BSA digest increased in intensity from 37.3 to 2135.2 (Figure 7b), indicating an enrichment factor of 57, and the other five detectable peptides in the original solution also increased 5.5 to 14.3-fold. The strongest peak (m/z = 1982) of the MYO digest increased in intensity from 34.5 to 2895.7 (Figure S7b, Supporting Information), showing an enrichment factor of 84, and the other two detectable peptides in the original solution also got a 15.4-fold increase and a 4.8-fold increase. The

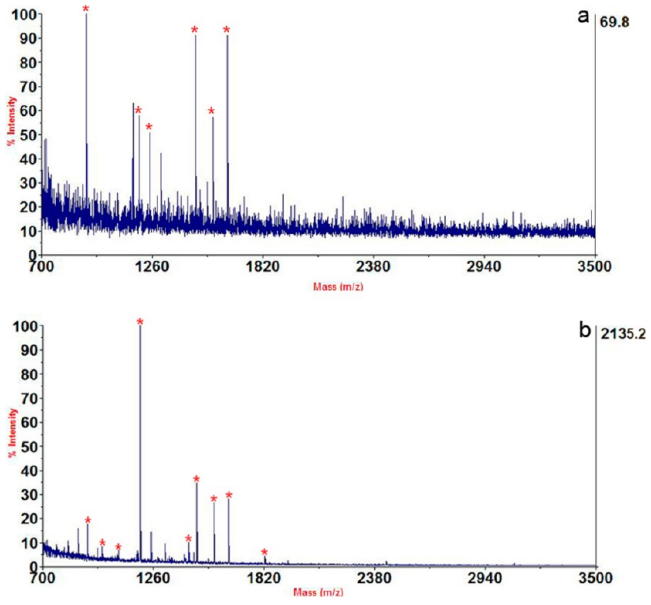

Figure 7. MALDI-TOF mass spectrum of 10 nM BSA digest (a) without any treatment and (b) after enrichment with magG@PDA@Cu^{2+}. The peaks marked with asterisks represent peptides of the BSA digest.

only matched peptide in Cytc digest rose from 74.9 to 889.7 in the S/N ratio (Figure S8b, Supporting Information), exhibiting an enrichment factor of 11.9. Such high enrichment factors were rare in previous reports dealing with the pretreatment of complex samples. Take the BSA digest solution as an example; Fe_3O_4@$nSiO_2$@$mSiO_2$ microspheres enhanced the S/N ratio of the peptides with the highest intensity (m/z = 927) for about 9.6 times,[42] C_8-functionalized Fe_3O_4@CP microspheres enhanced the S/N ratio of the peptides with the highest intensity (m/z = 927) for 11.5 times,[8] C60-f-MS enhanced the S/N ratio of the peptides with the highest intensity (m/z = 1640) for nearly 12.2 times.[10]

Tables S2, S3 and S4 (Supporting Information) display the search results of BAS, MYO and Cytc tryptic digests by using MASCOT server, the GRAVY value and theoretical isoelectric point (pI) of peptides assignable to the three tryptic digests. As is shown in Tables S2, S3 and S4 (Supporting Information), magG@PDA@Cu^{2+} composites could enrich hydrophilic and hydrophobic peptides ranging in GRAVY from −1.700 to +1.171. From the perspective of pI, magG@PDA@Cu^{2+} composites were more likely to enrich peptides with a theoretical pI lower than 8.3. Because the immobilization for IMAC is based on the principles of hard and soft acids and bases[43] and the enrichment procedure was performed in alkaline solution (pH = 8.3), the peptides with low pI values became negatively charged under this condition, increasing the chances to interact with the positively charged Cu^{2+}.

Human urine is easily obtained noninvasively for clinical diagnosis, so the application of magG@PDA@Cu^{2+} to the enrichment and identification of peptides in human urine is of great significance. To examine the feasibility of the enrichment method for more complicated mixtures, we spiked Angiotensin II to undiluted human urine, and its final concentration was adjusted to 20 and 10 nM. When the urine solutions were directly analyzed without enrichment (Figure 8a,c), no peptide could be identified with poor spectrum. Figure 8b,d depicts the mass spectra of the samples after treatment with magG@PDA@Cu^{2+}, the peak of Angiotensin II was successfully indentified with a S/N

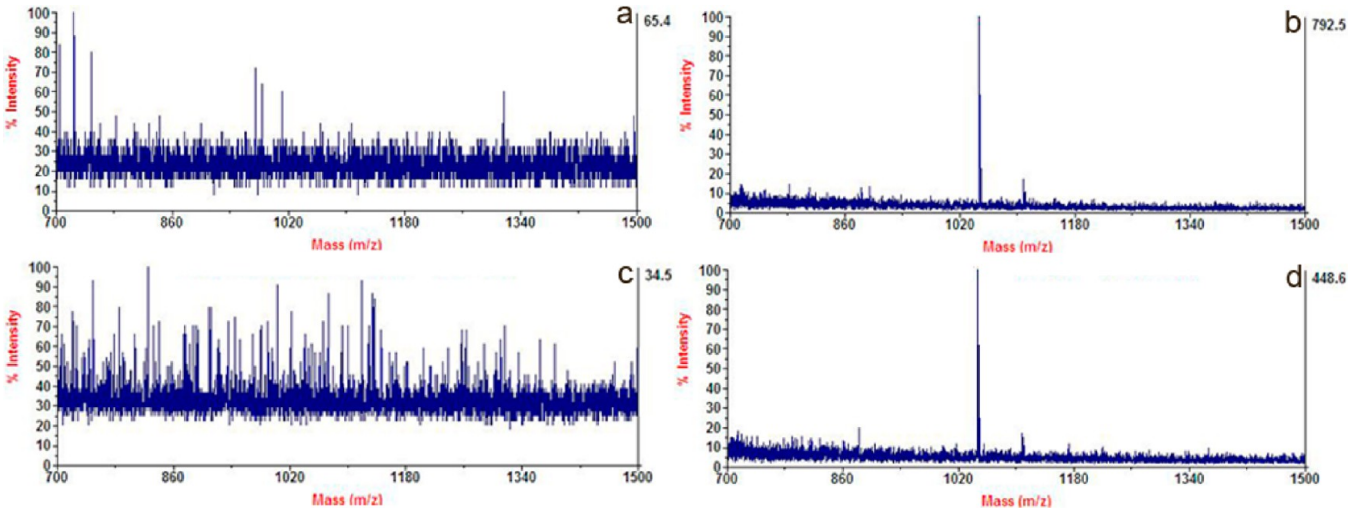

Figure 8. MALDI-TOF mass spectra of 20 and 10 nM Angiotensin II urine solution (a, c) without any treatment and (b, d) after enrichment with magG@PDA@Cu^{2+}.

ratio of 792.5 and 448.6 in 20 and 10 nM urine solutions. Besides, some endogenous peptides could also be observed. On the other hand, insulin, as the most critical indicator of the function of endocrine beta cells, was studied as a typical hydrophilic peptide to estimate the applicability of magG@PDA@Cu^{2+} for hydrophilic peptides in real samples. Insulin was dissolved in undiluted human urine, and its concentration was tuned to 20 and 10 nM. Being treated with magG@PDA@Cu^{2+} led to an increase in the S/N ratio from null to 2197.3 and 1400.8 (Figure S9, Supporting Information). Thus, magG@PDA@Cu^{2+} is expected to be an elegant alternative as the probe for concentrating and separating both hydrophobic and hydrophilic biomarkers from biological samples. In addition, magG@PDA@Cu^{2+} is also applicable in human serum (see Figure S10, Supporting Information), implying its universality in the practical pretreatment of samples.

CONCLUSIONS

In summary, in this study, the magnetic graphene was successfully coated with polydopamine via spontaneous oxidative polymerization of dopamine for the first time and the polydopamine-encapsulated magnetic graphene was easily modified with Cu^{2+} ions. We applied the Cu^{2+}-immobilized polydopamine-encapsulated magnetic graphene composites in the enrichment of low-concentration peptides. The novel magnetic material showed a high enrichment efficiency not only for standard hydrophilic and hydrophobic peptides but also for peptides in complex systems such as protein digests and peptides in human urine and serum. The novel composites possess the merits of ultrahigh surface area of graphene, high magnetic responsiveness of magnetite, biological compatibility and excellent dispersibility of polydopamine and strong affinity of Cu^{2+} ions toward peptides, thus allowing the enrichment and separation procedures to be performed conveniently and efficiently. Furthermore, it is likely to be a probe for concentrating and separating endogenous peptides from biological samples. The dopamine-based hybrid composites are expected to open up new horizons for the identification of low-abundance peptides and the detection of critical molecules in the human body that reflect the pathological state of certain diseases.

ASSOCIATED CONTENT

Supporting Information

Additional experimental details, XRD patterns of magG@PDA, EDX spectrum of magG@PDA@Cu^{2+}, zeta potential distributions of HNO_3-treated graphene, magG, magG@PDA and mag@PDA@Cu^{2+}, images of graphene and magG@PDA@Cu^{2+} dispersions and additional MALDI-TOF MS spectra. This material is available free of charge via the Internet at http://pubs.acs.org.

AUTHOR INFORMATION

Corresponding Author

*Prof. C. Deng. E-mail: chdeng@fudan.edu.cn. Fax: 86-21-65641740.

Notes

The authors declare no competing financial interest.

ACKNOWLEDGMENTS

This work was supported by the National Basic Research Priorities Program (2012CB910602, 2013CB911201), the National Natrual Science Foundation of China (21075022, 20875017, 21105016), Research Fund for the Doctoral Program of Higher Education of China (20110071110007, 20100071120053) and Shanghai Leading Academic Discipline Project (B109)

REFERENCES

(1) Mann, M.; Hojrup, P.; Roepstorff, P. *Biol. Mass Spectrom.* **1993**, *22*, 338−345.
(2) Yates, J. R.; Speicher, S.; Griffin, P. R.; Hunkapiller, T. *Anal. Biochem.* **1993**, *214*, 397−408.
(3) Fields, S. *Science* **2001**, *291*, 1221−1224.
(4) Abbott, A. *Nature* **2001**, *409*, 747−747.
(5) Diamandis, E. P. *J. Proteome Res.* **2006**, *5*, 2079−2082.
(6) Petricoin, E. F.; Belluco, C.; Araujo, R. P.; Liotta, L. A. *Nat. Rev. Cancer* **2006**, *6*, 961−967.
(7) Chen, H. M.; Xu, X. Q.; Yao, N.; Deng, C. H.; Yang, P. Y.; Zhang, X. M. *Proteomics* **2008**, *8*, 2778−2784.
(8) Chen, H. M.; Deng, C. H.; Li, Y.; Dai, Y.; Yang, P. Y.; Zhang, X. M. *Adv. Mater.* **2009**, *21*, 2200−2205.
(9) Liu, S. S.; Li, Y.; Deng, C. H.; Mao, Y.; Zhang, X. M.; Yang, P. Y. *Proteomics* **2011**, *11*, 4503−4513.

(10) Chen, H. M.; Qi, D. W.; Deng, C. H.; Yang, P. Y.; Zhang, X. M. *Proteomics* **2009**, *9*, 380−387.
(11) Liu, S. S.; Chen, H. M.; Lu, X. H.; Deng, C. H.; Zhang, X. M.; Yang, P. Y. *Angew. Chem., Int. Ed.* **2010**, *49*, 7557−7561.
(12) Novoselov, K. S.; Geim, A. K.; Morozov, S. V.; Jiang, D.; Zhang, Y.; Dubonos, S. V.; Grigorieva, I. V.; Firsov, A. A. *Science* **2004**, *306*, 666−669.
(13) Stoller, M. D.; Park, S. J.; Zhu, Y. W.; An, J. H.; Ruoff, R. S. *Nano Lett.* **2008**, *8*, 498−3502.
(14) Nayak, T. R.; Andersen, H.; Makam, V. S.; Khaw, C.; Bae, S.; Xu, X. F.; Ee, P. L. R.; Ahn, J. H.; Hong, H. B.; Pastorin, G.; Ozyilmaz, B. *ACS Nano* **2011**, *5*, 4670−4678.
(15) Kim, Y. K.; Kim, M. H.; Min, D. H. *Chem. Commun.* **2011**, *47*, 3195−3197.
(16) Lee, D. Y.; Khatun, Z.; Lee, J. H.; Lee, Y. K. *Biomacromolecules* **2011**, *12*, 336−341.
(17) Dong, X. L.; Cheng, J. S.; Li, J. H.; Wang, Y. S. *Anal. Chem.* **2010**, *82*, 6208−6214.
(18) Chen, J. M.; Zou, J.; Zeng, J. B.; Song, X. H.; Ji, J. J.; Wang, Y. R.; Ha, J.; Chen, X. *Anal. Chim. Acta* **2010**, *678*, 44−49.
(19) Chandra, V.; Park, J.; Chun, Y.; Lee, J. W.; Hwang, I. C.; Kim, K. S. *ACS Nano* **2010**, *4*, 3979−3986.
(20) Liu, Q.; Shi, J. B.; Sun, J. T.; Wang, T.; Zeng, L. X.; Jiang, G. B. *Angew. Chem., Int. Ed.* **2011**, *50*, 5913−5917.
(21) Cong, H. P.; He, J. J.; Lu, Y.; Yu, S. H. *Small* **2010**, *6*, 169−173.
(22) Liu, Q.; Shi, J. B.; Cheng, M. T.; Li, G. L.; Cao, D.; Jiang, G. B. *Chem. Commun.* **2012**, *48*, 1874−1876.
(23) Yin, P.; Wang, Y. H.; Li, Y.; Deng, C. H.; Zhang, X. M.; Yang, P. Y. *Proteomics* **2012**, *12*, 2784−2791.
(24) Herlinger, E.; Jameson, R. F.; Linert, W. *J. Chem. Soc., Perkin Trans. 2* **1995**, *2*, 259−263.
(25) Kang, S. M.; Rho, J.; Choi, I. S.; Messersmith, P. B.; Lee, H. *J. Am. Chem. Soc.* **2009**, *131*, 13224−13225.
(26) Lee, H.; Rho, J.; Messersmith, P. B. *Adv. Mater.* **2009**, *21*, 431−434.
(27) Kim, S. J.; Park, C. B. *Langmuir* **2010**, *26*, 14730−14736.
(28) Rao, C. N. R.; Sood, A. K.; Subrahmanyam, K. S.; Govindaraj, A. *Angew. Chem., Int. Ed.* **2009**, *48*, 7752−7777.
(29) Zheng, T. T.; Zhang, R.; Zou, L. F.; Zhu, J. J. *Analyst* **2012**, *137*, 1316−1318.
(30) Hu, H. Y.; Yu, B.; Ye, Q.; Gu, Y. S.; Zhou, F. *Carbon* **2010**, *48*, 2347−2353.
(31) Fei, B.; Qian, B. T.; Yang, Z. Y.; Wang, R. H.; Liu, W. C.; Mak, C. L.; Xin, J. H. *Carbon* **2008**, *46*, 1792−1828.
(32) Shi, C. Y.; Deng, C. H.; Zhang, X. M.; Yang, P. Y. *ACS Appl. Mater. Interfaces* **2013**, *5*, 7770−7776.
(33) Yang, S. H.; Kang, S. M.; Lee, K. B.; Chung, T. D.; Lee, H.; Choi, I. S. *J. Am. Chem. Soc.* **2011**, *133*, 2795−2797.
(34) Wang, J. L.; Ren, K. F.; Chang, H.; Jia, F.; Li, B. C.; Ji, Y.; Ji, J. *Macromol. Biosci.* **2013**, *13*, 483−493.
(35) Liu, Y. L.; Ai, K.; Liu, J. H.; Deng, M.; He, Y. Y.; Lu, L. H. *Adv. Mater.* **2013**, *25*, 1353−1359.
(36) Ou, J. F.; Wang, J. Q.; Zhang, D.; Zhang, P. L.; Liu, S.; Yan, P. H.; Liu, B.; Yang, S. R. *Colloids Surf., B* **2010**, *76*, 123−127.
(37) Zhang, M.; Zhang, X. H.; He, X. W.; Chen, L. X.; Zhang, Y. K. *Nanoscale* **2012**, *4*, 3141−3147.
(38) Farnad, N.; Farhadi, K.; Voelcker, N. H. *Water, Air, Soil Pollut.* **2012**, *223*, 3535−3544.
(39) Shi, C. Y.; Meng, J. R.; Deng, C. H. *Chem. Commun.* **2012**, *48*, 2418−2420.
(40) Liebscher, J.; Mrowczynski, R.; Scheidt, H. A.; Filip, C.; Hadade, N. D.; Turcu, R.; Bende, A.; Beck, S. *Langmuir* **2013**, *29*, 10539−10548.
(41) Chen, H. M.; Liu, S. S.; Li, Y.; Deng, C. H.; Zhang, X. M.; Yang, P. Y. *Proteomics* **2011**, *11*, 890−897.
(42) Chen, H. M.; Liu, S. S.; Yang, H. L.; Mao, Y.; Deng, C. H.; Zhang, X. M.; Yang, P. Y. *Proteomics* **2010**, *10*, 930−939.
(43) Oshima, T.; Tachiyama, H.; Kanemaru, K.; Ohe, K.; Baba, Y. *Sep. Purif. Technol.* **2009**, *70*, 79−86.